UMERC+OREC 2025 Conference

12-14 August | Corvallis, OR USA

WEC optimization to maximize grid economic value and avoided emissions

Rebecca McCabe[a 1], Madison Dietrich[a], Jiarui Yang[a],
Anthony Long[a], Khai Xin Kuan[b], Leah Buccino[a], Alan Liu[c], Maha Haji[a,d]

[a]*Sibley School of Mechanical and Aerospace Engineering, Cornell University, 124 Hoy Road, Ithaca, NY 14853, USA*
[b]*Cornell University Department of Information Science, 236 Gates Hall, Ithaca NY 14853, USA*
[c]*Cornell University Department of Economics, 109 Tower Road, Ithaca, NY 14853, USA*
[d]*Department of Systems Engineering, Cornell University, 136 Hoy Road, Ithaca, NY 14853, USA*

Abstract

Wave energy converter (WEC) design optimization has traditionally focused on minimizing the Levelized Cost of Energy (LCOE) or similar proxies. However, this approach overlooks the reality of energy system planning, where capacity installation decisions are made to minimize total grid cost. Grid system cost does not necessarily align with LCOE due to the complex temporal and spatial relationship between energy generation and demand. Additionally, conventional WEC optimization neglects broader climate and electrification goals, where the reduction of lifetime equivalent CO_2 emissions is the key metric. To bridge this gap, the authors previously proposed a system-level techno-economic and environmental WEC optimization framework that integrates capacity expansion modeling (CEM) and life cycle analysis (LCA) into the design objective. This approach provides a more comprehensive assessment of wave energy's net value proposition beyond conventional cost metrics. In this work, we implement this methodology in a new open-source multidisciplinary design optimization framework. Our implementation leverages the GenX CEM, the PowerGenome energy data interface, the Idemat LCA dataset, and the MDOcean WEC model. A surrogate model of the CEM reduces computation time compared to the naive CEM-in-the-loop approach, leveraging a reduced order model to shrink the relevant design space from 18 dimensions to just 5. A second order pole-zero reduced order model is compared to the nonlinear dynamics simulation and found to be valid only at frequencies at and below resonance. An alternative hydrodynamics-informed reduced order model is proposed to capture the full dynamics with lower order, but is not yet implemented. We present preliminary CEM results for the Reference Model 3 (RM3) WEC, demonstrating that a 30% reduction in WEC capacity cost can lead to a 10% reduction in grid system cost and a 20% reduction in CO_2 emissions for the Northeast grid. The LCA model also suggests that to be environmentally viable, each MWh of energy the WEC generates must displace around 0.1-0.2 MWh of fossil fuels, a target which the nominal RM3 does not achieve.Full design optimization results are pending and will demonstrate the impact of optimizing for new value-driven economic and environmental system metrics compared to the standard LCOE.

Keywords: techno-economic model, environmental impact assessment, energy grid integration, multidisciplinary design optimization, life cycle analysis, capacity expansion model

[1]∗ Corresponding author. E-mail address: rgm222@cornell.edu

1 Introduction

Advances in wave energy converter (WEC) multidisciplinary design optimization show potential to reduce Levelized Cost of Energy (LCOE) by > 50% [1]. However, LCOE does not fully capture WEC value [2, 3]. Alternative metrics include payback period for off-grid contexts [4], net value of energy and profitability in single-technology economic evaluation [2, 5], and grid system cost and CO_2 emissions in energy system planning and climate change mitigation [3]. Prior WEC grid studies reveal benefits of reduced curtailment, higher capacity factor, and improved grid reliability due to seasonal complementarity with solar, proximity to coastal load, and wave resource consistency [6, 7, 8].

Considering energy system factors in the early design phase can steer WEC development to leverage this value, maximizing climate benefit. Recent studies for other technologies incorporate design considerations into grid optimization [9, 10], grid considerations into design optimization [11], and combined grid and environmental considerations into design optimization [12, 13]. This study is the first to apply integrated design and grid optimization to WECs, and is a methodological improvement over similar work. Specifically, a surrogate capacity expansion model (CEM) within a nonlinear design optimization more fully captures design-grid coupling and is computationally efficient.

2 Methodology

2.1 *Optimization problem formulation*

The WEC being optimized is the Reference Model 3 (RM3) point absorber [14]. We utilize MDOcean [15], an open-source WEC design optimization framework, with the same design variables and constraints as [1]. The twelve design variables include five bulk geometric dimensions (float and spar diameter and height, and float-spar vertical clearance), two generator ratings (power and force), and five structural dimensions (float, spar, and damping plate material thicknesses, and float and damping plate stiffener height). See [1] for variable ranges and rationales. Constraints include pitch stability, hydrostatic balance, structural survival, and dynamic amplitude limits. New in this study, the primary optimization objective is CEM grid cost. To avoid flatness, the objective becomes the margin to viability if the WEC is not economically viable. To capture system environmental impacts, we add a second new objective of net eco-value per energy. Figure 1 depicts the optimization structure in an xDSM diagram [16], with design variables on the top, objectives and constraints in the rightmost two columns, and simulation modules along the diagonal.

2.2 *Modeling*

MDOcean integrates hydrodynamic, structural, control, and economic models, detailed in [1]. This study introduces new "grid" and "environment" modules to MDOcean. Grey lines in Figure 1 show module connections. As [17] proposes, we perform CEM optimizations before the design optimization for a wide set of inputs that reflect the range of possible WEC designs and parameters. The grid module of the design optimization captures CEM results in a surrogate model to reduce computation time, enabled by a reduced order dynamics model. Using a CEM rather than historical grid data correlations means that we accurately account for marginal generators, unlike prior work [12, 13].

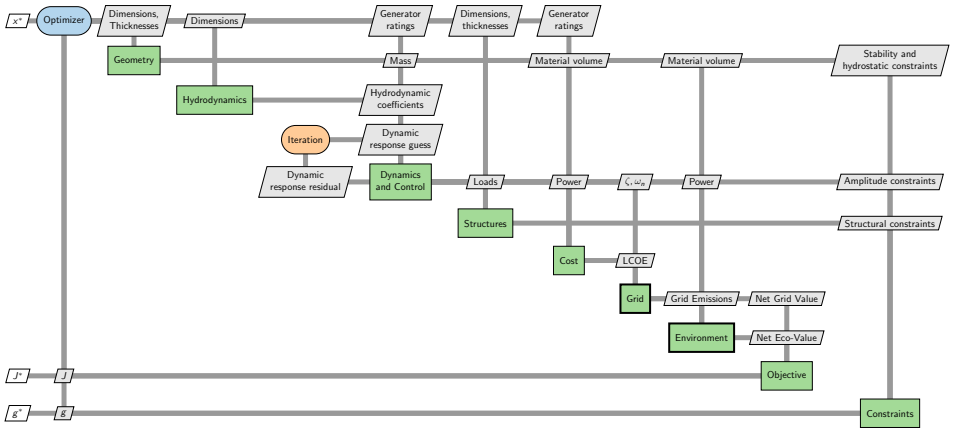

Figure 1: xDSM diagram

2.2.1 *Capacity expansion model (CEM)*

The GenX CEM [18] is an open-source linear program that determines the installed capacity of each generator to minimize the total grid system cost while meeting demand and emissions constraints. It indirectly enforces economic equilibrium since it is optimal to only install generators that cost less than the value they provide. This implies that NVOE (net value of electricity), a metric which [2, 17] suggest, is always zero in a CEM. The CEM grid system cost metric captures more effects than NVOE, such as costs and avoided costs of non-WEC generators, storage, and transmission required to balance the grid given the WEC power profile. GenX requires detailed input data on the cost, hourly profile, and existing infrastructure of all generation, transmission, storage, and load on the grid. This is managed by the PowerGenome package [19], which consolidates data from multiple sources including scenarios for reference, moderate, and high levels of electrification. PowerGenome also allows control over a grid-wide maximum CO_2 constraint. Figure 2 depicts the data flow for the CEM runs prior to design optimization and documents the grid data sources. Grid costs and emissions are found for each input combination of WEC cost, grid scenario, location, and WEC dynamics (damping ratio and natural frequency). Orange outlines indicate code implemented in this work rather than an existing package. PowerGenome does not provide WEC data, so we use the MHKit interface [20] to NREL hindcast power densities [21, 22] along with design-dependent capture width information to generate the WEC hourly power profiles. Temporal and spatial resolution and scope are set to hourly energy profiles for one year each decade for a Northeast grid scenario with three load zones.

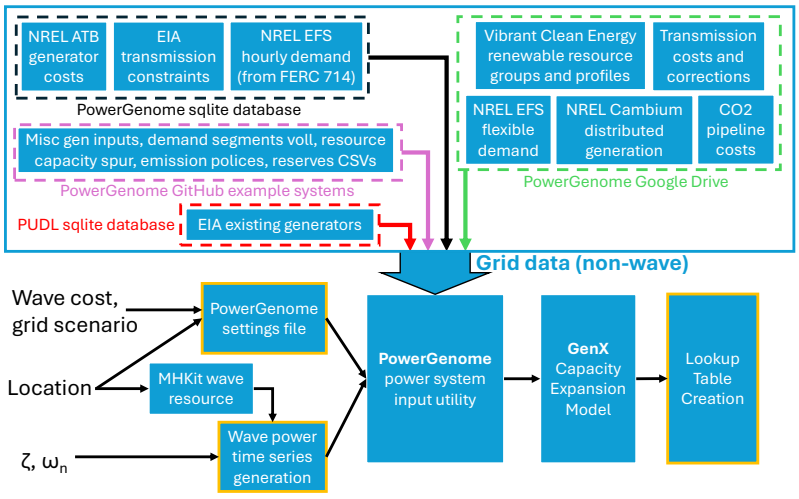

Figure 2: CEM data flow

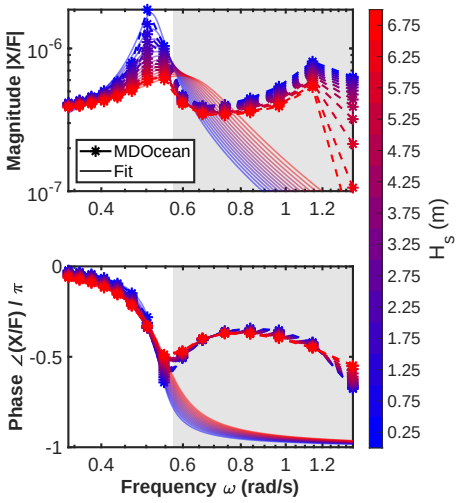

Figure 3: Second order Bode fit

2.2.2 *Reduced order model and lookup table*

The two WEC inputs to the CEM are capacity cost and power profile (hourly energy density times capture width CW at matching wave heights and periods). Cost can be swept easily, but $CW(H_s, T_e)$ depends on 15 additional inputs. A 16-dimensional sweep is computationally prohibitive, so we use a reduced order model (ROM) to collapse the WEC design space into a few key features and a surrogate model to predict CEM outputs from the reduced space. The ROM is used only to capture the effect of WEC design on the hourly CEM variability profile, not to calculate energy.

First we nondimensionalize to reduce the design space. The $CW(H_s, T_e)$ equation has 18 quantities: CW, H_s, T_e, 6 design variables, and 9 parameters. The Buckingham-π theorem reduces this to 15 dimensionless variables $\mathbf{\Pi_1}$ without approximation (see Appendix A). To further reduce, we leverage rigid body dynamics, which dictates the following:

$$\frac{CW}{CW_{max}} = \frac{4\mathcal{D}\eta_{PTO}}{G}\frac{\omega^2}{gk}\frac{\Re(\hat{Z}_h(\mathbf{\Pi_1}))\,\Re(\hat{Z}_u(\mathbf{\Pi_1}))}{\left|\hat{Z}_h(\mathbf{\Pi_1}) + \hat{Z}_u(\mathbf{\Pi_1}) + \hat{Z}_d(\mathbf{\Pi_1})\right|^2} \tag{1}$$

where complex impedances $\hat{Z}$ have subscript u for control, h for hydrodynamic radiation, and d for drag. $\mathcal{D}$ is defined in the appendix. The ROM seeks to approximate the three functions $\hat{Z}(\mathbf{\Pi_1})$ as functions of a reduced set of values $\mathbf{\Pi_2}$.

Before the design optimization, the CEM is run for all combinations of $\mathbf{\Pi_2}$. During design optimization, we perform a least-squares fit over an error model to find the reduced groups $\mathbf{\Pi_2}$ at each iteration, and then use a surrogate model to find CEM outputs as a function of $\mathbf{\Pi_2}$. Currently, the surrogate model is a lookup table with linear interpolation. Future work could develop a mechanistic surrogate model to understand CEM driving factors and allow extrapolation to different grid scenarios.

Two approaches are possible in selecting $\mathbf{\Pi_2}$ and the corresponding error model: a pole-zero description of the dynamics to obtain a low-order transfer function, or a hydrodynamics-informed curve fit. A pole-zero description, $\mathbf{\Pi_{2,pz}}$, is easy to implement via standard system identification tools, but may require a high order to adequately capture the dynamics. A variety of existing WEC models use this [23] or similar approaches [24]. Appendix A shows the equation for an arbitrary number of poles and zeros. Alternatively, a custom hydrodynamics curve fit, $\mathbf{\Pi_{2,hyd}}$, offers more accuracy at lower order using deep mechanistic understanding of the physics. Appendix A shows a fit to describe radiation impedance $\hat{Z}_h$ as a function of kh using only two parameters.

This study evaluates a second-order pole-zero model $\mathbf{\Pi_{2,pz}} = (\zeta, \omega_\mathbf{n})$ to fit the closed loop system compliance, $\hat{X}/\hat{F} = 1/(i\omega(\hat{Z}_h + \hat{Z}_u + \hat{Z}_d))$, but finds a poor fit. Specifically, Figure 3 shows that for the nominal RM3, the model is valid only at frequencies at and below resonance. Capturing behavior above resonance would require a higher order model such as one with five poles, two standard zeros, and two right half plane zeros to capture the abrupt increase in phase. This is similar to another study where a point absorber intrinsic impedance $\hat{Z}_h + \hat{Z}_d$ was fit with three poles and one right half plane zero [23]. However, sweeping this many dynamic inputs to the CEM is impractical, and high frequencies are less common in the ocean, so here we maintain a second order model and exclude frequencies with $\omega > 0.6$ from the fit (shown in grey). Fitting each wave height separately lets the model capture drag nonlinearities, which manifest as a roughly locally linear dependence of ζ and ω_n on wave height. Figure 4 shows this relation when fitting magnitude and phase separately. The magnitude fit depends significantly more on H_s than the phase fit. Mismatch of magnitude and phase fits at low H_s is evidence of a nonminimum phase system, and the larger mismatch at high H_s is due to drag nonlinearities. While it doesn't affect the shape of $\hat{Z}(\omega)$, stiffness K also shows nonlinearity.

Difficulty capturing high-frequency behavior is expected from the model structure. A second-order system has equivalent damping $B = \Re(\hat{F}/(i\omega\hat{X})) = 2\zeta/\omega_n$, which is constant across frequency, and equivalent reactance $K - (m + A)/\omega^2 = \Re(\hat{F}/\hat{X}) \sim 1 - \omega^2/\omega_n^2$, which only permits added mass frequency-dependence of the form $A = A_\infty + A_0/\omega^2$ [25]. This does not align with the true shape of $\hat{Z}_h(\omega)$, in which B decreases (perhaps after an initial increase) and A often has local minima and maxima. Future work should better explore hydrodynamic curve fits $\mathbf{\Pi_{2,hyd}}$.

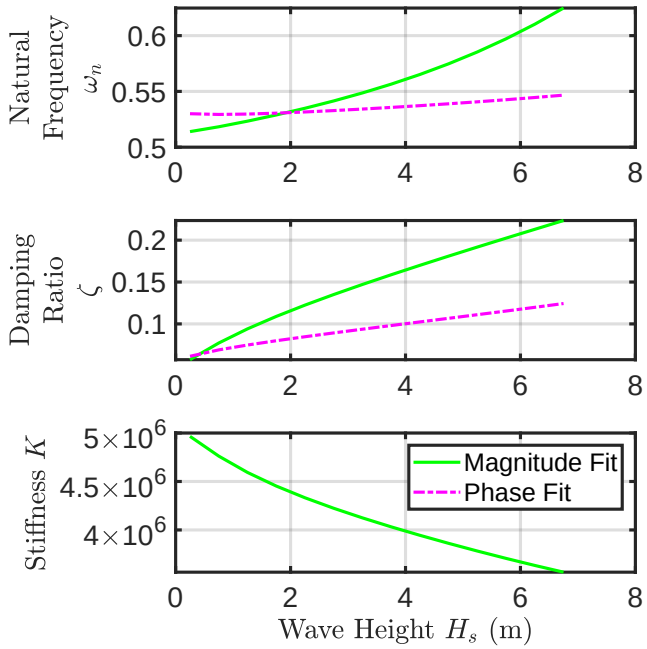

Figure 4: Variation of fit parameters with wave height

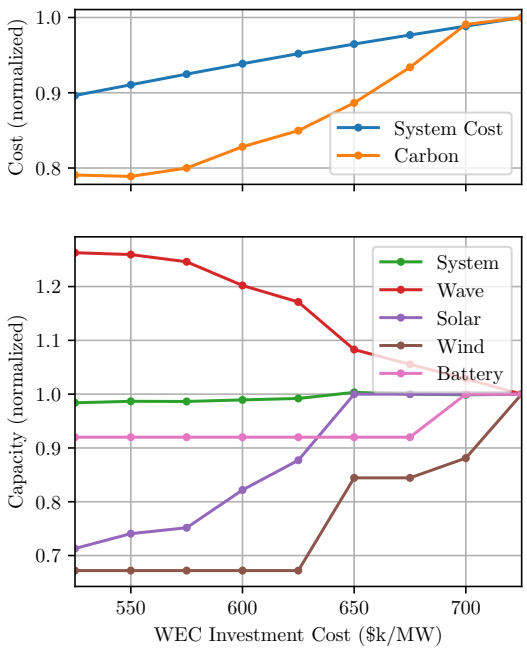

Figure 5: CEM cost sweep for ISONE

2.2.3 *Life cycle analysis (LCA)*

LCA in the early design phase is challenging due to uncertainties in materials, manufacturing, and transportation [26]. Fortunately, optimization only requires modeling effects that meaningfully scale with design variables. This includes material use (steel, fiberglass) but not aquatic habitat disruption or hydraulic fluid toxicity since they are not captured in MDOcean's low design fidelity. Although the present study holds distance from shore constant, the environmental model includes offshore transportation (diesel fuel) so future work can evaluate the tradeoff between better energetics but worse survivability, operating cost, and maintenance emissions for WECs further offshore.

MDOcean's geometry module calculates WEC material masses and the environment module multiplies by appropriate weighting coefficients from the Idemat LCA dataset [27]. These are scope 3 eco-cost coefficients [28] that express diverse lifetime environmental impacts (i.e. water, emissions, pollution) of various materials and processes in monetary units (see Table 1). We convert Euros to USD via the March 2024 exchange rate of 1.09 \$/€. MDOcean then offsets the eco-cost with the eco-value of CEM avoided grid emissions using the social cost of carbon. Finally, it normalizes by CEM WEC grid energy production to obtain the net eco-value per unit energy (\$/kWh).

Component	Value
Steel	0.192 \$/kg
Fiberglass	6.950 \$/m^2
Dist. from shore	65.88 \$/mile
Social cost of CO_2	0.145 \$/kgCO_2

Table 1: Eco-cost coefficients

The nominal RM3 eco-cost is \$134,800 per WEC. 95% is from steel, 5% from fiberglass, and <1% from transportation. Using the social cost of carbon, each WEC must displace >930 tonnes of CO_2 emissions on the grid over its lifetime to "break even" (achieve a net positive eco-value). With an annual energy production of 500 MWh and 20 year lifetime, it must displace 0.093 tonnes of CO_2 per MWh. Typical natural gas and coal plants emit around 0.5 and 1.0 tonnes of CO_2 per MWh respectively. Therefore, for each MWh of energy that RM3 generates, it must displace at least 0.18 MWh of natural gas or 0.09 MWh of coal to have a positive net eco-value.

3 Results and conclusions

It took 20 minutes to run the 15 CEM optimizations on an Ubuntu 20.04 server with Intel(R) Core(TM) i9-10940X CPU @ 3.30GHz, using up to 28 threads for each optimization and executing successive optimizations in series. Of this time, only around half is spent in GenX, since PowerGenome takes 35 seconds per case. Figure 5 shows the normalized grid cost, CO2 emissions, and capacity from the CEM for a WEC with $\zeta = 0.05, \omega_n = 0.4$, and $B_u = 10^5 \omega e^{-\omega^2}$ (a Rayleigh distribution: an alternative model to the one in Appendix A) in the Northeast. As the WEC gets cheaper (moving from right to left), the grid cost, emissions, and capacity of other renewables reduce as expected, and WEC capacity increases. Capacity behaves nonlinearly: cheaper WECs first displace wind, then batteries, then solar. The different "cut-in costs" to displace each technology likely reflect both capital costs and power profiles. The x-axis width of the cut-in reflects the heterogeneity of each resource. For example, the batteries displaced are very homogeneous, with all sites having a cut-in cost of 675-700 \$k/MW, but wind and solar have a wide range of cut-in costs due to resource variation across sites. Unlike capacity, system cost varies linearly with WEC cost. The slope has a useful sensitivity interpretation: for every 30% WEC cost reduces, system cost reduces 10%. Meanwhile, emission reduction is moderately linear with WEC cost, but appears more strongly linear with WEC capacity. The most expensive designs have a ratio of fossil fuel energy displaced to WEC energy produced of 0.075, below the 0.09-0.18 requirement. Even if RM3 was economically viable, it does not avoid enough emissions to be environmentally viable. This shows the importance of both economic and environmental considerations in design optimization.

Further examination of the time-series results is required to understand if WECs in this system primarily derive value from seasonal balancing, consistency, availability at peak times, or some other characteristic. Additionally, sweeping all design parameters and grid scenarios remains necessary to populate the lookup table for design optimization, and to more broadly understand the grid value of WECs' unique temporal power profile and its dependence on design. Future work could examine the sensitivity of CEM results to the resource and demand data year to avoid overfitting, especially since wave resource data is not aggregated across sites as PowerGenome does for wind and solar. Finally, design optimization results will yield insight into whether and how the objective values and optimal design features meaningfully vary when optimizing for LCOE, grid cost, or net eco-value across various grid scenarios.

Acknowledgments and Data Availability

We thank Olivia Vitale and Collin Treacy for feedback on a draft. Open-source code: design optimization at `github.com/symbiotic-engineering/MDOcean` and CEM at `github.com/symbiotic-engineering/wec-decider`.

Appendix A. Reduced order model details

The $CW(H_s, T_e)$ equation initially involves 18 quantities: CW, H_s, T_e, 6 design variables (generator ratings F_{lim} and P_{lim} and float and spar diameters D_f and D_s and drafts T_f and T_s), and 9 parameters (damping plate diameter and thickness D_d and h_d, efficiency η_{PTO}, float and spar drag coefficient $C_{d,f}$ and $C_{d,s}$, damping versus reactive control type C, water depth h, water density ρ, and acceleration of gravity g). These span three physical dimensions (length, time, and mass). By the Buckingham-π theorem, the relationship can be reduced to a function of $18 - 3 = 15$ dimensionless groups [29]. Capture width is nondimensionalized by the maximum radiative capture width, $CW_{max} = Gg/\omega^2$, with gain G (1 for heave, 2 for surge/pitch) and frequency ω [30]. Wave height is divided by water depth. Wave period is captured as the product of wavenumber and water depth, kh. Generator force and power limits are nondimensionalized by the force and power at the maximum capture width, F_{max} and P_{max}. The six dimensions are divided by each other or the water depth.The efficiency, drag coefficients, and control type are already nondimensional. Thus, we have the following $\mathbf{\Pi_1}$ dimensionless groups:

$$\frac{CW}{CW_{max}} = f(\mathbf{\Pi_1}) = f\left(\frac{H_s}{h}, kh, \frac{P_{lim}}{P_{max}}, \frac{F_{lim}}{F_{max}}, \frac{D_f}{h}, \frac{D_s}{D_f}, \frac{T_f}{T_s}, \frac{T_s}{h}, \frac{D_d}{D_f}, \frac{t_d}{D_d}, \eta_{PTO}, C_{d,f}, C_{d,s}, C\right) \tag{2}$$

Moving to the pole-zero ROM, a general model with C_P complex pole pairs, C_Z complex zero pairs, R_P real poles, and R_Z real zeros has a total of $2C_P + 2C_Z + R_P + R_Z$ parameters and is expressed as:

$$\mathbf{\Pi_{2,pz}} = \left(\zeta_p,\ \omega_{n,p},\ \zeta_z,\ \omega_{n,z},\ \tau_p,\ \tau_z\right), \quad \frac{\hat{X}}{\hat{F}} = \prod_{r_p=1}^{R_P}\prod_{r_z=1}^{R_Z}\prod_{c_p=1}^{C_P}\prod_{c_z=1}^{C_Z} \frac{1+\tau_{z,r_z} i\omega}{1+\tau_{p,r_p} i\omega} \times \frac{1-\left(\frac{\omega}{\omega_{n,c_z}}\right)^2 + i2\zeta_{c_z}\frac{\omega}{\omega_{n,c_z}}}{1-\left(\frac{\omega}{\omega_{n,c_p}}\right)^2 + i2\zeta_{c_p}\frac{\omega}{\omega_{n,c_p}}} \tag{3}$$

The pole-zero ROM tested in the paper uses $C_P = 1, C_Z = R_P = R_Z = 0$.

Alternatively, the following custom hydrodynamics curve fits radiation impedance as a function of kh using only two parameters, kD_f and B_0^e. The latter is approximated as constant, neglecting frequency and geometry dependence:

$$\mathbf{\Pi_{2,hyd}} = (kh, kD_f, B_0^e), \quad \frac{\hat{F}}{\eta} = \frac{-4i\rho g h\sqrt{N_0}B_0^e}{\cosh(kh)\, H_0(kD_f/2)}, \quad B_h = \frac{k\omega\,|\hat{F}/\eta|^2}{2\mathcal{D}\rho g^2}, \quad A = \frac{1}{\pi\omega}\,\text{p.v.}\int_0^\infty \frac{B(t)}{t - kD_f/2}dt \tag{4}$$

The $\hat{F}/\eta$ equation leverages the eigenfunction form of the excitation coefficient for axisymmetric bodies, where H_0 is the Hankel function and $N_0 = \frac{1}{2}\left(1 + \frac{\sinh(2kh)}{2kh}\right)$ [31]. The B_h equation applies the Haskind relation to obtain the damping, where $\mathcal{D} = \tanh(kh) + kh(1 - \tanh^2(kh))$ [31]. The A equation applies the Kramers-Kronig relation to obtain the added mass, where p.v. is Cauchy principal value [32]. Note that (4) only yields a fit for $\hat{Z}_h$ and does not attempt to capture the effect of drag nonlinearities ($\hat{Z}_d$) or impedance mismatch due to force limit, power limit, or damping control ($\hat{Z}_u$), although it is expected that mechanistic curve fits for these effects could be developed using only 2-3 additional parameters, as opposed to the 5 such groups in $\mathbf{\Pi_1}$.

References

[1] Rebecca McCabe, Madison Dietrich, and Maha Haji. *Leveraging Multidisciplinary Design Optimization and Semi-Analytical Modeling to Advance Wave Energy Converter Viability*. 2025.

[2] Matthew Mowers and Trieu Mai. "An evaluation of electricity system technology competitiveness metrics: The case for profitability". In: *The Electricity Journal* 34.4 (May 1, 2021), p. 106931. ISSN: 1040-6190. DOI: 10.1016/j.tej.2021.106931. URL: https://www.sciencedirect.com/science/article/pii/S1040619021000221 (visited on 10/30/2023).

[3] Jill Moraski, Malwina Qvist, and Kasparas Spokas. *Beyond LCOE: A Systems-Oriented Perspective for Evaluating Electricity Decarbonization Pathways*. Clean Air Task Force, May 2025. URL: https://www.catf.us/resource/beyond-lcoe/ (visited on 07/01/2025).

[4] Scott Jenne. *Powering the Blue Economy: Economics of Marine Renewable Energy Systems*. NREL/PR-5700-78328. National Renewable Energy Lab. (NREL), Golden, CO (United States), July 29, 2021. URL: https://www.osti.gov/biblio/1811994 (visited on 03/07/2023).

[5] Elaheh Makaremi. "Economic Evaluation Metrics for Energy Island Solutions, including wind and wave energy generation systems". Accepted: 2025-06-27T16:41:58Z. Master thesis. University of South-Eastern Norway, 2025. URL: https://openarchive.usn.no/usn-xmlui/handle/11250/3202262 (visited on 07/01/2025).

[6] Kerem Ziya Akdemir et al. "Opportunities for wave energy in bulk power system operations". In: *Applied Energy* 352 (Dec. 15, 2023), p. 121845. ISSN: 0306-2619. DOI: 10.1016/j.apenergy.2023.121845. URL: https://www.sciencedirect.com/science/article/pii/S0306261923012096 (visited on 06/02/2024).

[7] Saptarshi Bhattacharya et al. "Timing value of marine renewable energy resources for potential grid applications". In: *Applied Energy* 299 (Oct. 1, 2021), p. 117281. ISSN: 0306-2619. DOI: 10.1016/j.apenergy.2021.117281. URL: https://www.sciencedirect.com/science/article/pii/S030626192100698X (visited on 01/31/2025).

[8] Shona Pennock et al. "Temporal complementarity of marine renewables with wind and solar generation: Implications for GB system benefits". In: *Applied Energy* 319 (Aug. 1, 2022), p. 119276. ISSN: 0306-2619. DOI: 10.1016/j.apenergy.2022.119276. URL: https://www.sciencedirect.com/science/article/pii/S030626192200633X (visited on 01/31/2025).

[9] Jacob A. Schwartz et al. "The value of fusion energy to a decarbonized United States electric grid". In: *Joule* 7.4 (Apr. 19, 2023). Publisher: Elsevier, pp. 675–699. ISSN: 2542-4785, 2542-4351. DOI: 10.1016/j.joule.2023.02.006. URL: https://www.cell.com/joule/abstract/S2542-4351(23)00075-2 (visited on 05/22/2023).

[10] Wilson Ricks, Jack Norbeck, and Jesse Jenkins. "The value of in-reservoir energy storage for flexible dispatch of geothermal power". In: *Applied Energy* 313 (May 1, 2022), p. 118807. ISSN: 0306-2619. DOI: 10.1016/j.apenergy.2022.118807. URL: https://www.sciencedirect.com/science/article/pii/S0306261922002537 (visited on 05/15/2023).

[11] Mihir Kishore Mehta, Michiel Zaaijer, and Dominic von Terzi. "Designing wind turbines for profitability in the day-ahead market". In: *Wind Energy Science* 9.12 (Dec. 5, 2024). Publisher: Copernicus GmbH, pp. 2283–2300. ISSN: 2366-7443. DOI: 10.5194/wes-9-2283-2024. URL: https://wes.copernicus.org/articles/9/2283/2024/ (visited on 07/01/2025).

[12] Helena Canet, Adrien Guilloré, and Carlo L. Bottasso. "The eco-conscious wind turbine: design beyond purely economic metrics". In: *Wind Energy Science* 8.6 (June 23, 2023). Publisher: Copernicus GmbH, pp. 1029–1047. ISSN: 2366-7443. DOI: 10.5194/wes-8-1029-2023. URL: https://wes.copernicus.org/articles/8/1029/2023/ (visited on 07/01/2025).

[13] S Kainz, A Guilloré, and C L Bottasso. "How do technological choices affect the economic and environmental performance of offshore wind farms?" In: *Journal of Physics: Conference Series* 2767.8 (June 2024). Publisher: IOP Publishing, p. 082005. ISSN: 1742-6596. DOI: 10.1088/1742-6596/2767/8/082005. URL: https://dx.doi.org/10.1088/1742-6596/2767/8/082005 (visited on 07/01/2025).

[14] Vincent S Neary et al. *Methodology for Design and Economic Analysis of Marine Energy Conversion (MEC) Technologies*. SAND2014-9040. Albuquerque, New Mexico: Sandia National Laboratories, Mar. 2014, p. 262. URL: https://energy.sandia.gov/wp-content/gallery/uploads/SAND2014-9040-RMP-REPORT.pdf.

[15] Rebecca McCabe et al. *MDOcean*. Version v2.1. Oct. 27, 2024. DOI: 10.5281/zenodo.13997244. URL: https://zenodo.org/records/13997244 (visited on 01/02/2025).

[16] Andrew B. Lambe and Joaquim R. R. A. Martins. "Extensions to the design structure matrix for the description of multidisciplinary design, analysis, and optimization processes". In: *Structural and Multidisciplinary Optimization* 46.2 (Aug. 1, 2012), pp. 273–284. ISSN: 1615-1488. DOI: 10.1007/s00158-012-0763-y. URL: https://doi.org/10.1007/s00158-012-0763-y (visited on 01/23/2025).

[17] Rebecca McCabe et al. "System Level Techno-Economic and Environmental Design Optimization for Ocean Wave Energy". In: ASME International Design Engineering Technical Conferences. Boston, MA, USA, Aug. 20, 2023.

[18] Luca Bonaldo et al. *GenXProject/GenX.jl: v0.4.4*. Feb. 5, 2025. DOI: 10.5281/zenodo.14807684. URL: https://zenodo.org/records/14807684 (visited on 06/30/2025).

[19] Greg Schivley et al. *PowerGenome/PowerGenome: v0.7.0*. Mar. 21, 2025. DOI: 10.5281/zenodo.15066032. URL: https://zenodo.org/records/15066032 (visited on 06/30/2025).

[20] Katherine Klise et al. *MHKiT (Marine and Hydrokinetic Toolkit) - Python*. Published: [Computer Software] https://doi.org/10.5281/zenodo.3924683. Jan. 2020. DOI: 10.5281/zenodo.3924683. URL: https://doi.org/10.5281/zenodo.3924683.

[21] Wei-Cheng Wu et al. "Development and validation of a high-resolution regional wave hindcast model for U.S. West Coast wave resource characterization". In: *Renewable Energy* 152 (June 1, 2020), pp. 736–753. ISSN: 0960-1481. DOI: 10.1016/j.renene.2020.01.077. URL: https://www.sciencedirect.com/science/article/pii/S0960148120300963 (visited on 07/02/2025).

[22] M. Nabi Allahdadi et al. "Development and validation of a regional-scale high-resolution unstructured model for wave energy resource characterization along the US East Coast". In: *Renewable Energy* 136 (June 1, 2019), pp. 500–511. ISSN: 0960-1481. DOI: 10.1016/j.renene.2019.01.020. URL: https://www.sciencedirect.com/science/article/pii/S0960148119300175 (visited on 07/02/2025).

[23] Giorgio Bacelli et al. "System Identification of a Heaving Point Absorber: Design of Experiment and Device Modeling". In: *Energies* 10.4 (Apr. 2017). Number: 4 Publisher: Multidisciplinary Digital Publishing Institute, p. 472. ISSN: 1996-1073. DOI: 10.3390/en10040472. URL: https://www.mdpi.com/1996-1073/10/4/472 (visited on 07/14/2025).

[24] Erlend Kristiansen, Åsmund Hjulstad, and Olav Egeland. "State-space representation of radiation forces in time-domain vessel models". In: *Ocean Engineering* 32.17 (Dec. 1, 2005), pp. 2195–2216. ISSN: 0029-8018. DOI: 10.1016/j.oceaneng.2005.02.009. URL: https://www.sciencedirect.com/science/article/pii/S0029801805000946 (visited on 07/14/2025).

[25] G.F. Franklin, J.D. Powell, and A. Emami-Naeini. *Feedback control of dynamic systems*. Always learning. Pearson, 2014. ISBN: 978-1-292-06890-9. URL: https://books.google.com/books?id=y02hoAEACAAJ.

[26] Sheikh Moniruzzaman Moni et al. "Life cycle assessment of emerging technologies: A review". In: *Journal of Industrial Ecology* 24.1 (2020). _eprint: https://onlinelibrary.wiley.com/doi/pdf/10.1111/jiec.12965, pp. 52–63. ISSN: 1530-9290. DOI: 10.1111/jiec.12965. URL: https://onlinelibrary.wiley.com/doi/abs/10.1111/jiec.12965 (visited on 03/04/2023).

[27] Jasper van den Herik and Joost Vögtlander. *Idemat scope 3 eco-costs*. Version 2024. 2024. URL: https://www.ecocostsvalue.com/data-tools-books/ (visited on 04/15/2024).

[28] Joost G Vogtlander et al. *LCA-based assessment of sustainability: the Eco-costs/Value Ratio (EVR)*. Sustainable Design Series of Delft University of Technology. Oegetgeest, The Netherlands: Sustainability Impact Metrics, 2010. URL: https://www.ecocostsvalue.com/EVR/img/references%20ecocosts/Book_EVR.pdf.

[29] Garreth McKinley, W Cheng, and John Brisson. "Dimensional Analysis". In: *2.006: Thermal Fluids Engineering II*. Spring 2021. Cambridge, MA: MIT CopyTech, 2021, p. 78.

[30] Shangyan Zou, Bryson Robertson, and Solomon Yim. "Practical power absorption assessment limits for generic wave energy converters". In: *Ocean Engineering* 277 (June 1, 2023), p. 114303. ISSN: 0029-8018. DOI: 10.1016/j.oceaneng.2023.114303. URL: https://www.sciencedirect.com/science/article/pii/S002980182300687X (visited on 12/22/2024).

[31] Fun Pang Chau and Ronald W. Yeung. "Inertia, Damping, and Wave Excitation of Heaving Coaxial Cylinders". In: ASME 2012 31st International Conference on Ocean, Offshore and Arctic Engineering. American Society of Mechanical Engineers Digital Collection, 2012, pp. 803–813. DOI: 10.1115/OMAE2012-83987. URL: https://dx.doi.org/10.1115/OMAE2012-83987 (visited on 09/28/2023).

[32] M. Greenhow and S. I. Ahn. "Added mass and damping of horizontal circular cylinder sections". In: *Ocean Engineering* 15.5 (Jan. 1, 1988), pp. 495–504. ISSN: 0029-8018. DOI: 10.1016/0029-8018(88)90012-1. URL: https://www.sciencedirect.com/science/article/pii/0029801888900121 (visited on 07/14/2025).